Journal of Nano Research Vol. 23 (2013) pp 74-82
Online available since 2013/Jul/29 at www.scientific.net

doi:10.4028/www.scientific.net/JNanoR.23.74

Energy Absorption in Gold Nanoshells

Changhong Liu[1, 2,a] and Ben Q. Li[3,b]

[1]Department of Electrical Engineering, Shanghai Jiao Tong University, China

[2]School of Mechanical Engineering, Xi'an Jiaotong University, China

[3]Department of Mechanical Engineering, University of Michigan-Dearborn, U.S.

[a]liuch@sjtu.edu.cn, [b]benqli@umich.edu

[Submitted: Jan. 12, 2013; revised: April 21, 2013; accepted: April 24, 2013]

Keywords: nanoshell, energy, absorption, plasmon resonance, intercoupling.

Abstract. A modeling study on energy absorption and transport in an isolated nanoshell and aggregates of nanoshells under localized surface plasma resonance (SPR) conditions is presented. A comprehensive model for multi-scattering of electromagnetic waves by a cluster of multilayered nanoshells is developed, which applies the Wigner-Eckart theorem for the calculation of the total scattering cross sessions of nanoshell aggregates. Absorption by an isolated nanoshell and by nanoshell clusters is studied using the model. Results show that the inter-nanoshell coupling results in strong field enhancement near the particle surface. Energy absorption in a nanoshell can be tuned by varying the structural parameters of the nanoshell. Smaller particles are more absorbing than the large ones, other conditions being equal. Because of the presence of a dielectric cavity, the radial distribution of the absorbed power in the metal shell may differ from the classical skin depth phenomena. The interaction among particles in close proximity causes the energy absorption efficiency and the resonance position of a nanoshell cluster to differ from those of an isolated nanoshell.

Introduction

Gold nanoshells have found applications in a wide range of optical and thermal systems [1-6]. A key feature of the nanoshells critical to these applications is that the localized surface plasma resonance associated with these nanostructured particles is frequency-tunable by varying the ratio of shell thickness over the particle size. Making use of this key feature, one can design an efficient heat absorber, with identical nanoshells, that resonantly absorbs the light energy at a prescribed frequency. Alternatively, an efficient energy absorber can be made with an aggregate of nanoshells of various sizes, which resonantly absorb the light energy over a band of selected frequencies. Understanding of the fundamentals governing the energy transport and absorption in individual and aggregates of these types of nanostructures is of crucial importance for rational design of these nanostructures for thermal energy related applications.

Optical performance of individual and aggregate of nanoshells can be analyzed within the theoretical framework of the Mie solution, enhanced with the vector additional theorem for spherical harmonics [7-10]. To date, two most widely used approaches for simulating randomly orientated particles are the cluster T-matrix approach (CTM) [11] and the generalized multiparticle Mie-solution (GMM) [12]. Their similarities and differences were compared by Xu [13]. Besides these rigorous analytical solutions for aggregated particles, the approximate methods, e.g. the discrete dipole approximation (DDA) [14] and finite difference time domain methods (FDTD) [15] are also used in the numerical computation of light scattering, especially for the systems involving irregular geometries. Of course, the DDA and FDTD methods have their limitations [16]. For randomly distributed multilayered nanoshells, analytical solutions are superior to DDA and FDTD from the standpoint of both calculation time and accuracy. However, it is not exaggerated to state that to date the multi-scattering simulation models, either analytical or numerical, have not yet been developed to the level where they satisfy all the practical needs. In a recent publication, the authors

have presented a computational model by combining the recursive algorithm with the vector addition theorem to study the multiscattering of electromagnetic waves by aggregate of multilayered nanostructures [17]. It appears that so far, much attention of the published work has been focused on the scattering of electromagnetic waves and relatively little attention has been paid to the aspect of energy absorption and transport in individual and aggregate of nanoshells. This paper discusses a modeling study of resonance absorption and transport in individual and aggregate of nanoshells when excited by a laser source.

Mathematical Model

The computational model used in this study has been presented in detail elsewhere [17] and thus only a brief outline is given here. The model is developed to describe multiscattering of electromagnetic waves by an individual or an ensemble of concentric spherical particles of different sizes and of different shell thicknesses positioned at different locations. It solves the vector form of the Maxwell equations,

$$\nabla^2\mathbf{E} + k^2\mathbf{E} = 0 \tag{1}$$

where **E** is the electric field and $k^2 = \omega^2\varepsilon\mu = \omega m/c$ with c being the speed of light, m the refractive index, ε the electric permittivity, ω the angular frequency, and μ the magnetic permeability.

The computational procedure starts with a recursive algorithm for the Mie solution for an isolated multilayered nanoshell. The nanoshell is essentially a spherical particle of L concentric layers, with each layer characterized by a size parameter $x_l = 2\pi\tilde{N}_l\, r_l\, /\lambda$ and a relative refractive index $m_l = \tilde{N}_l/\tilde{N}$, where λ is wavelength, r_l and $\tilde{N}_l$ are radius and refractive index of the l^{th} layer (l = 1, 2, …, L), and $\tilde{N}$ is refractive index of the host media. By means of spherical eigenvectors, the electromagnetic field inside the l^{th} layer is expanded as

$$\mathbf{E}_l = \sum_{n=1}^{\infty} E_n \left[c_n^l \mathbf{M}_{o1n}^{(1)} - i d_n^l \mathbf{N}_{e1n}^{(1)} + i a_n^l \mathbf{N}_{e1n}^{(3)} - b_n^l \mathbf{M}_{o1n}^{(3)} \right] \tag{2}$$

where c_n and d_n are the coefficients of the wave functions for the internal field and are calculated recursively and for an plane incident wave, $E_n = i^n E_0 (2n+1)/n(n+1)$.

For an aggregate of multilayered nanoshells, the scattered electromagnetic field for the i^{th} nanoshell in the aggregate takes the following form,

$$\mathbf{E}_s(j) = \sum_{n=1}^{\infty} \sum_{m=-n}^{n} (a_{mn}^j \mathbf{m}_{mn}^{(3)}(j) + b_{mn}^j \mathbf{n}_{mn}^{(3)}(j)) \tag{3}$$

where $a_{mn}^j = -p_{mn}^j \beta_n^{j,(L+1)}$ and $b_{mn}^j = -q_{mn}^j \alpha_n^{j,(L+1)}$ are the scattering coefficients, p_{mn}^j, q_{mn}^j are the coefficients for the applied incident plane wave, and $\alpha_n^{j,(L+1)}$ and $\beta_n^{j,(L+1)}$ are scattering wave coefficients for the j^{th} nanoshell .

By the vector addition theorem, the scattered field of the i^{th} particle written for its coordinates is translated into the incident field for the j^{th} particle with the coordinates fixed at the j^{th} particle by the following transformations,

$$\begin{aligned} \mathbf{m}_{mn}^{(3)}(i) &= \sum_{\mu=1}^{\infty} \sum_{\nu=-\mu}^{\mu} \left(A_{mn}^{\mu\nu}(i,j) \mathbf{m}_{\mu\nu}^{(1)}(j) + B_{mn}^{\mu\nu}(i,j) \mathbf{n}_{\mu\nu}^{(1)}(j) \right) \\ \mathbf{n}_{mn}^{(3)}(i) &= \sum_{\mu=1}^{\infty} \sum_{\nu=-\mu}^{\mu} \left(B_{mn}^{\mu\nu}(i,j) \mathbf{m}_{\mu\nu}^{(1)}(j) + A_{mn}^{\mu\nu}(i,j) \mathbf{n}_{\mu\nu}^{(1)}(j) \right) \end{aligned} \tag{4}$$

where (i) means that the wave functions **m** and **n** are written in the coordinates fixed at the i^{th} nanoshell, and the coefficients for the transformation are $A_{mn}^{\mu\nu}(i,j)$ and $B_{mn}^{\mu\nu}(i,j)$ given in [18].

After the transformation has been applied to all nanoshells in the aggregate, the boundary conditions at the outer surface of the j^{th} nanoshell yield the expressions for the coefficients of the scattered field of the j^{th} nanoshell as related to the same coefficients of other nanoshells. This procedure results in a system of equations with the scattered field coefficients for each nanoshell being the unknowns, which can be solved by matrix inversion.

The total extinction cross section of the cluster is given by

$$C_{ext} = \frac{4\pi}{k^2}\sum_{n}^{\infty}\sum_{m=\pm 1}\frac{n(n+1)}{2n+1}\frac{(n+m)!}{(n-m)!}(p_{mn}^{0*}a_{mn}^{T} + p_{mn}^{0*}b_{mn}^{T}) \tag{5}$$

where the total scattering coefficients of the cluster, a_{mn}^{T} and b_{mn}^{T} are calculated by

$$\begin{pmatrix} a_{mn}^{T} \\ b_{mn}^{T} \end{pmatrix} = \begin{pmatrix} a_{mn}^{j_0} \\ b_{mn}^{j_0} \end{pmatrix} + \sum_{\substack{j=1 \\ j\neq j_o}}^{N}\sum_{\nu=1}^{\infty}\sum_{\mu=\pm 1}\left(\begin{pmatrix} a_{\mu\nu}^{j} \\ b_{\mu\nu}^{j} \end{pmatrix} a_{\mu\nu}^{j} A'^{\mu\nu}_{mn}(j,j_o) + \begin{pmatrix} b_{\mu\nu}^{j} \\ a_{\mu\nu}^{j} \end{pmatrix} B'^{\mu\nu}_{mn}(j,j_o) \right) \tag{6}$$

Here the center of the j_0th sphere is taken as the origin of the cluster, the coefficients $A'^{\mu\nu}_{mn}$ and $B'^{\mu\nu}_{mn}$ are the translation coefficients.

The total scattering cross section could also be calculated in terms of a_{mn}^{T} and b_{mn}^{T}; however, its numerical accuracy can suffer for certain particle arrangements. To overcome the difficulty, an expression that makes the direct use of the scattering coefficients for each particle the aggregate is derived [19],

$$\begin{aligned} C_{sca} = \frac{4\pi}{k^2}\sum_{n}^{\infty}\sum_{m=-n}^{n}\sum_{l}^{L}\Bigg(& (a_{mn}^{l}a_{mn}^{*l} + b_{mn}^{l}b_{mn}^{*l})\frac{n(n+1)}{2n+1}\frac{(n+m)!}{(n-m)!} + \\ & + 2\,\mathrm{Re}\sum_{\nu}^{\infty}\sum_{\mu=-\nu}^{\mu=\nu}\sum_{\lambda>l}^{L}[(a_{mn}^{l}a_{\mu\nu}^{*\lambda} + b_{mn}^{l}b_{\mu\nu}^{*\lambda})C_{mn\mu\nu} + (b_{mn}^{l}a_{\mu\nu}^{*\lambda} + a_{mn}^{l}b_{\mu\nu}^{*\lambda})D_{mn\mu\nu}]\Bigg) \end{aligned} \tag{7}$$

$$C_{mn\mu\nu} = \frac{(-1)^{\mu+n}}{2}\frac{(n+m)!}{(n-m)!}\sum_{p=|n-\nu|}^{n+\nu} i^{p+n+\nu}c(m.n,\mu,\nu,p)j_p(ku_{\lambda l})P_p^{m-\mu}(\cos\theta_{\lambda l})e^{i(m-\mu)\varphi_{\lambda l}} \tag{8}$$

$$c(m.n,\mu,\nu,p) = [n(n+1)+\nu(\nu+1)-p(p+1)]\frac{(p-m+\mu)!}{(p+m-\mu)!}a(-m,n,\mu,\nu,p) \tag{9}$$

The original form of $D_{mn\mu\nu}$ is rather complex and a more compact form of it may be obtained using the Wigner-Eckart theorem [18],

$$\begin{aligned} D_{mn\mu\nu} = (-1)^{\mu+1}\sum_{p=|n-\nu|}^{n+\nu} i^{\nu-n+p}\frac{1-(-1)^{p+n+\nu}}{2}(2p+1)\begin{pmatrix} p & n & \nu \\ 0 & 1 & -1 \end{pmatrix}\begin{pmatrix} p & n & \nu \\ -m+\mu & m & -\mu \end{pmatrix}\sqrt{\frac{(\nu+\mu)!}{(\nu-\mu)!}\frac{(n+m)!}{(n-m)!}\frac{(p-m+\mu)!}{(p+m-\mu)!}} \\ j_p(\kappa r)P_p^{m-\mu}(\cos\theta_R)e^{i(m-\mu)\varphi_R} \end{aligned} \tag{10}$$

Note that $D_{mn\mu\nu} = 0$ if $p+n+\nu = even$. The absorption cross section for the i^{th} particle in the aggregate can be calculated by the following expression,

$$C_{abs}^{i} = \frac{4\pi}{k^2\,|\,m_l^i\,|^2}\,\mathrm{Re}\sum_{n=1}^{\infty}\sum_{m=-1}^{m=1} i\frac{n(n+1)}{2n+1}\frac{(n+m)!}{(n-m)!}\left(C_1^i + C_2^i + C_3^i\right) \tag{11}$$

where

$$C_1^i = \psi_n\,'(m_L^i x_L^i)\psi_n^*(m^i x_L^i)(m^i c_{mn}^{i,(L)}c_{mn}^{*i,(L)} + m^{*i}d_{mn}^{i,(L)}d_{mn}^{*i,(L)}) \tag{12}$$

$$C_2^i = \xi_n\,'(m_L^i x_L^i)\xi_n^*(m_L^i x_L^i)(m^i b_{mn}^{i,(L)}b_{mn}^{*i,(L)} + m^{*i}a_{mn}^{i,(L)}a_{mn}^{*i,(L)}) \tag{13}$$

$$C_3^i = \sum_{l=1}^{\infty}\begin{Bmatrix} \mathrm{Re}[i\psi_n^*(m_L^i x_L^i)\xi_n'(m_L^i x_L^i)(mc_{mn}^{*i,L}b_{mn}^{i,L} + m^*d_{mn}^{*i,L}a_{mn}^{i,L})] + \\ \mathrm{Re}[i\psi_n\,'(m_L^i x_L^i)\xi_n^*(m_L^i x_L^i)(mc_{mn}^{i,L}b_{lmn}^{*i,L} + m^*d_{mn}^{i,L}a_{mn}^{*i,L})] \end{Bmatrix} \tag{14}$$

and coefficients c_{mn} and d_{mn} and be calculated in[20]. The total absorption cross section is given by $C_{abs} = C_{ext} - C_{sca} = \sum_l^L C_{abs}^l$. The internal field can now calculated using Eqs. (2) and (3). Knowing the internal field, one can determine the heat generation in a metal layer, which is the real part of the divergence of the Poynting vector.

Results and Discussions

To verify the computational methodology presented above, the scattering spectrum of an individual Au@SiO2 and a dimer are computed and compared with the reported measured spectral curves [21, 22]. The optical properties of gold are obtained from Johnson and Christy's paper [23], and modified to account for the intrinsic nanosize effect [24]. As is evident in Fig. 1, the calculated spectra are in excellent agreement with the experimental measurements, indicating that both the addition-theorem recursive computing scheme and accuracy criterion are gratifying.

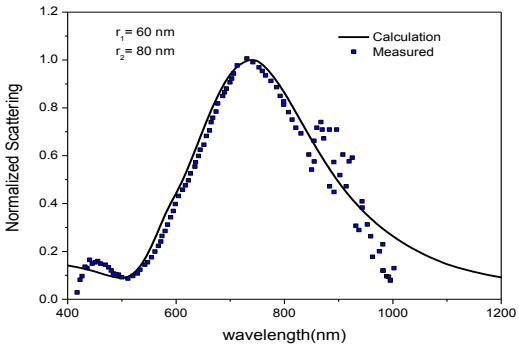

(a) Spectrum of an Au@silica nanoshell

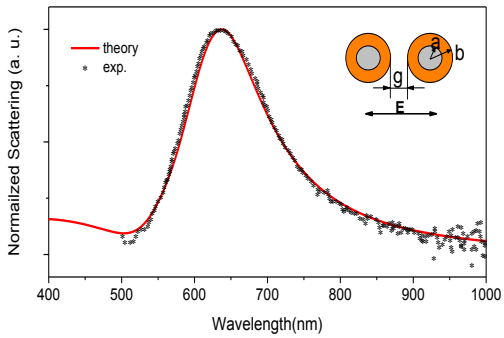

(b) Spectrum of an Au@silica dimer

Fig. 1 Verification of calculation. (a) Normalized scattering spectra of an Au@silica nanoshell. The inner and outer radii were indicated in the figure. The solid line is obtained by the recursive calculation described in this paper, and the dotted points are measured results, taken from [21]. (b) Normalized scattering spectra of an Au@silica dimer. The dimer axis is parallel to the electric field (parallel polarization). The silica core and gold shell are of 42nm radius and 17nm-thick, and particle space is 20nm. The experiment data comes from [22].

Absorption spectrum of an isolated nanoshell

Let us consider first the absorption of light by a single gold nanoshell within the region from VIS to NIR. Figure 2 shows the computed spectra of an isolated nanoshell, which has an outer radius from 40nm to 80nm, and shell thickness from 6nm to 12nm. The spectral curves were selected such that their surface plasma resonance (SPR) peak is ~800nm. It is seen from Fig.2 (a) that smaller particles are more absorbing than the larger ones. Moreover, the bigger the particle, the more predominant the higher order mode of the resonance becomes. Thus, for the optimal absorption of light, a small-sized particle is preferred over a larger one. Fig. 2(b) plots the corresponding scattering spectra of nanoshells mentioned in Fig. 2(a). It reveals that a larger particle scatters light more strongly. This implies that for thermal related applications, smaller-sized particles should be favored, while for scattering-based applications, bigger-sized particles with scattering component predominating in extinction should be used. In Table 1, the resonance wavelength and the percentage of absorption and scattering to the extinction are given for seven different nanoshells studied. For an integrated imaging and heating application, the particle with size 60:52nm appears to be better candidates, since the ratio of absorption efficiency (Qabs) to scattering efficiency (Qsca) of these particles is almost ~1:1.

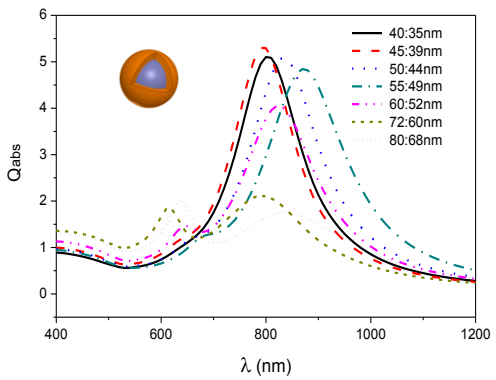

(a) Absorption spectra

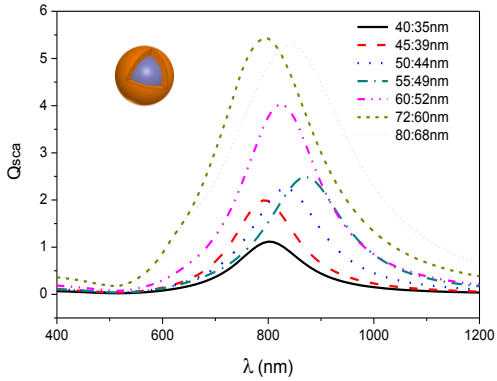

(b) Scattering spectra

Fig.2 Absorption and scattering spectrum vs. varying particle size.

Table 1. Extinction, absorption and scattering efficiency vs. structural dimensions of nanoshells

Particle Size(nm)	40:35	45:39	50:44	55:49	60:52	71.5:59.5	80:68
Resonance wavelength(nm)	800	790	840	870	820	795	840
Extinction Efficiency(Qext)	6.22	7.29	7.32	7.34	8.07	8.05	7.31
Qabs/Qext	82.2%	72.7%	69.3%	66.1%	50.1%	32.6%	27.6%
Qsca/Qext	17.8%	27.3%	30.7%	33.9%	49.9%	67.4%	72.4%

Power distribution in a nanoshell

Besides the overall absorption and scattering behavior of nanoshells, detailed heat generation and its distribution inside the conductive metal shell is also of importance to assess the local thermal environment. At present, to the best of our knowledge, thermal issues have been rarely reported compared to the exhausted literature on the scattering problems of particles. Figure 2 illustrates the absorbed power generation in and the energy distribution around an individual gold nanoshell of 72nm:60nm in size. The nanoshell is surrounded by water and illuminated by an x-polarized z-direction propagating plane wave. Figure 3(a) depicts the normalized energy distribution in the XOY cross section under resonance condition. Obviously, the strongest SPR-induced field enhancement occurs near the outer surface. Figure 3(b) shows the distribution of Joule heat in metal layer, which reveals that near the regions where the field enhancement is strongest, the heat generation inside the gold shell is the lowest. For example, in Fig. 2(a) the maximal field enhancement occurs at the two ends along x-axis, i.e. along the polarization direction. However, in the gold shell, the heat generation at these two ends attains a minimum. This can be explained by the fact that the applied external field is reversely superimposed with the polarization field inside the nanoshell, while outside the nanoshell, it is just the opposite. Figure 3(c) gives a three dimensional view of the distribution of Joule heat on the outermost spherical surface at dipole SPR mode. Clearly, the absorbed energy unevenly spreads in the metal layer with strong heating taking place around the equator.

The detailed radial distribution of absorbed energy is plotted in Fig. 3(d). It can be seen that the energy absorbed near the core-shell interface is even higher than that at the outer shell surface, in contrast with the well-known electromagnetic skin depth decay. This phenomenon is apparently a result of interaction between the electromagnetic wave and a nano-cavity. Light penetrating through the nano-sized shell into the cavity is confined within and undergoes repeated reflections by the cavity wall until they are absorbed by the metal, thereby giving rise to the non-classical profile. Further calculations show that this novel phenomenon appears to occur only in the nanoscaled structured particles, for instance, the nanoshells. For a solid Au nanoparticle, the energy distribution follows the classical behavior of exponential decay from the outer surface inward. The results presented here suggest that nanoshells are not only frequency-tunable but also absorption tunable. By the latter, it is meant that by changing the structural parameter of a nanoshell, one can significantly enhance the absorption while minimizing the scattering. This is an important feature that may be used to maximize the energy absorption for thermal applications**.**

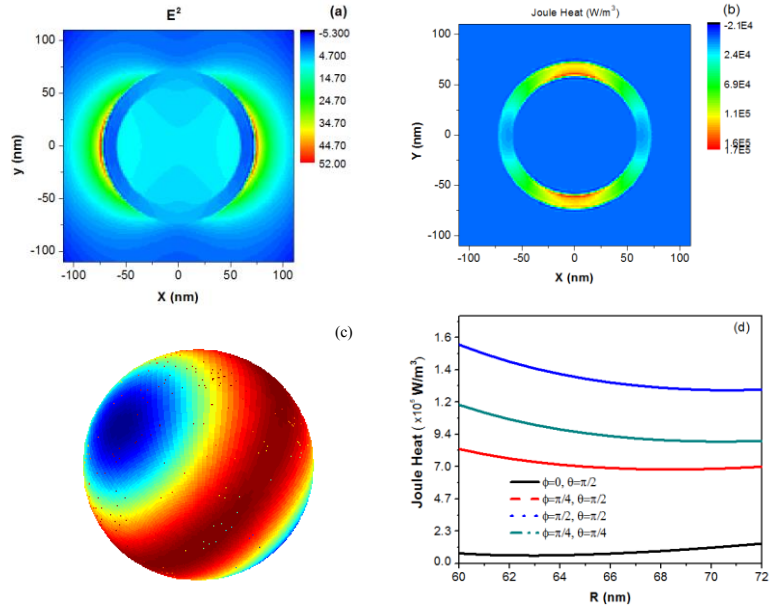

Fig. 3 The field enhancement and loss distribution in a gold nanoshell: (a) Energy contour in XOY plane at 795nm (b) Distribution of Joule heat within the gold shell, (c) 3-D distribution of Joule heat on the outer surface of gold shell, and (d) Joule heat along radial direction.

Effect of inter-particle coupling on absorption

In the above, energy absorption an isolated nanoshell is studied. Since nanoparticle aggregates are more realistic in practical applications, inter-particle interactions can affect the absorption properties of an individual gold nanoshell in the aggregate, and of a nanoshell aggregate.

In Figure 3, near field coupling effects are studied for an oriented nanodimer, which consists of two identical gold nanoshells. Figure 4(a) plots the absorption spectrum of a single nanoshell in the pair when the axis of nanodimer is aligned with polarization direction (parallel orientation hereafter). A series of interparticle separations, g=0, 0.25b, 0.5b, b, …, 4b, where *g* and *b* stand for the interparticle surface-to-surface gap and outer radius of the nanoshell, is considered. It is seen that when the two nanoshells are in contact, both dipole and quadrupole resonance shift towards a longer wavelength; moreover, the dipole resonance shits even more significantly than the quadrupole. In comparison with an isolated nanoshell, the maximum red-shift of dipole resonance goes up as much as 200nm. This significant red-shift is attributed to the interaction of the surface charges from the closely spaced nanoparticles. When the particles are aligned with the electric field vector, the negative charges of one particle are adjacent to the positive ones of the neighbor particle. The attractive force between opposite polarity charges limits the restoring force acted on the electrons, thereby resulting in a lower resonance frequency accordingly. The interparticle separation effect is also examined in Fig. 4(a). It is evident that by gradually increasing the separation between particles, the magnitude of absorption efficiency tends to approach that of an isolated nanoshell eventually, although the value oscillates nonlinearly along the way.

Figure 4(b) represents the case where the axis of nanodimer is normal to the polarization direction (normal orientation for short). As shown in the figure, when the two particles are fully in contact, Qabs is much lower than that of an isolated nanoshell. With an increase in interparticle separation, the maximum Qabs of the nanodimner starts to rise, and becomes even larger than that of an isolated particle at some specific separations. Similar situation occurs with the parallel orientation. It is also found that Qabs varies nonlinearly with interparticle separation. In comparison with the parallel case in Fig. 4(a), the resonance positions, of both dipole and quadruple, are always close to that of an isolated nanoshell, when the field is perpendicular to the dimer axis. Figure 4(c) plots the absorption spectra when the axis of nanodimer is parallel to the wave vector. In such an alignment, the absorption of the two nanoshells differs from each other. To be consistent with Fig.

4(a) and (b), the averaged absorption of the two nanoshells is used for discussion. It is seen that the average absorption efficiency of the nanodimer attains a maximum at g=0, almost three times as that of a single particle. Examination of the spectra over particle separations indicates that the magnitude of absorption cross section oscillates as g increases, sometimes higher than that of a single particle, while other times not. Nonetheless, the maximal absorption occurs when the particles are in touch along the direction of wave propagation. The resonance peaks are almost always around that of an isolated nanoshell over the entire range of interparticle separations.

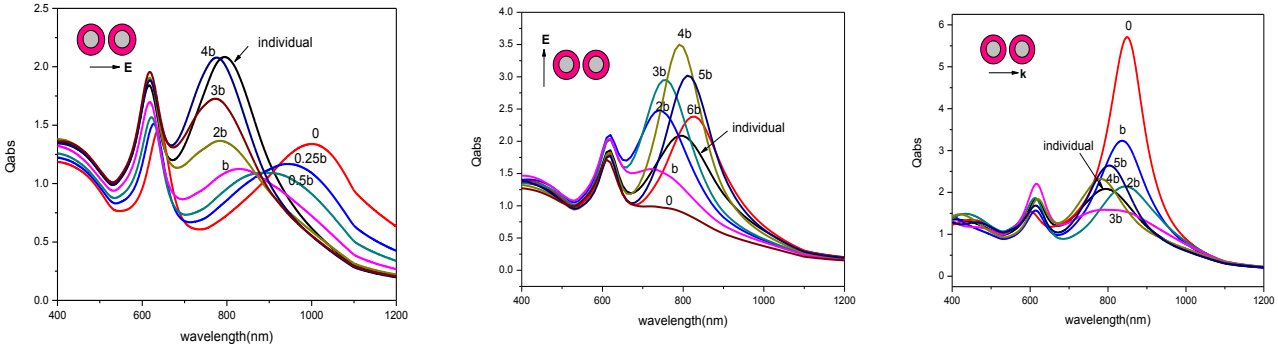

(a) Parallel orientation (b) Normal orientation (c) Wave orientation

Fig. 4 Absorption spectra of a nanodimer.

Energy absorbed by nanoshell aggregates

The modeling study is now extended to investigate the absorption by a nanoshell cluster or a group of clusters. Our laboratory experiments show that nanoshells, when made in solution, tend to cluster together due to the imbalance of electrostatic and the *van der Waals* force between particles. Model simulations were conducted for various scenarios and selected results are given in Fig. 5. The particles in the cluster are the same, all with 60nm-radius silica core, a 12nm-thick gold shell, and with three particles along each axial direction. The interpartice surface-to-surface distance (designated by *g*) is kept as a vaiable. The averaged absorption efficiency (total absorption efficiency divided by the total number of nanoparticle number, NT=7 in this case) is used. From Fig. 5(a), it is clear that both the resonance wavelength and the averaged absorption efficiency are different from the counterparts of an isolated nanoshell. This change in the total absorption is caused by the combined coupling effect as discussed in the previous section, that is, the electromagnetic coupling of nanoshells along the polarization direction results in a dominant red-shift in the collective resonance of a particle aggregate, while the interaction between particles perpendicular to polarization direction causes the resonance peak to shift only slightly. The magnitude of the absorption efficiency depends on the interparticle spacing, however.

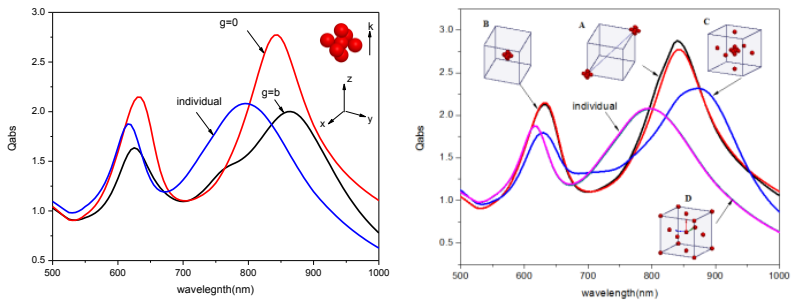

(a) One cluster (b) Two cluster

Fig.5 Absorption spectrum of aggregated nanoshells

The energy absorption by an assemble of 13~15 nanshells is calculated and given in Fig. 5(b) for different spatial arrangement within the same space volume. Curve A considers two clusters. The center-to-center spacing of the two clusters is 20b=1440nm. The average Qabs is compared with that of a single cluster (curve B) and of an isolated nanoshell. Since the spacing of the two clusters

is greater than one wavelength, the interaction between the clusters is insignificant. This is the reason why curve A is almost the same as curve B. Both curves, however, are different from that of an isolated nanoshell. In Case C, a center cluster is surrounded by the rest of the nanoshells uniformly dispersed. Finally, curve D is the case where one particle is at the center of the cube, and the other fourteen nanoshells spread at the vertex or the face center of the cube. It is found that the average absorption spectrum of group D almost coincides with that of individual nanoshell. This is attributed to the weak coupling effect due to large interparticle separations.

The results in Fig. 5 suggest that the aggregation of nanoshells can have a strong effect on the plasmonic absorption. Both absorption magnitude and resonance wavelength can differ from that of an individual particle considerably. This effect should be accounted for when specific thermal applications involving nanoshells are considered.

Summary

This paper has presented a modeling study of energy absorption and transport in gold nanoshells in isolation and in aggregates under localized surface plasma resonance conditions. A generalized theoretical formulation for multi-scattering of electromagnetic waves by multilayered nanoshells was employed to represent the scattering and absorption phenomena associated with nanoshells when excited by a light source. The model is further improved for its efficiency and accuracy by the use of Wigner-Eckart theorem for the calculation of the total scattering cross sessions of nanoshell aggregates. Absorption by an isolated nanoshell, a nanodimer, and nanoshell clusters was simulated using the model and analyzed. Results show that the coupling of the nanoshells results in strong field enhancement near the particle surface and that the SPR resonance peaks exhibit significant right shifts when the particles aligned along polarization direction. Energy absorption in a nanoshell can be tuned by varying the relative structural parameters of the nanoshell. Smaller particles are more absorbing than the large ones, other conditions being equal. Because of the presence of cavity, the radial distribution of the absorbed power in the metal shell may differ from the classical skin depth phenomena, with the maximum absorbed power occurring at the inner surface of the metal shell. The energy absorption in nanoshell aggregates depends on the interparticle spacing. The interaction among particles in close proximity causes the energy absorption behavior of clusters to differ considerably from that of an isolated nanoshell, in both the magnitude of absorption efficiency and the resonance position.

Acknowledgments

We gratefully acknowledge the financial support of Shanghai Natural Science Foundation (11ZR1417300), Shanghai Jiao Tong University Project (YG2011MS25) and Key Laboratory of Pressure and Safety (MOE), East China University of Science and Technology.

References

[1] C. Loo, L. Hirsch, and M.H. Lee, *Optical Letters,* 30 (2005)1012-1014.

[2] L. B. Carpin, L. R. Bickford, G. Agollah, T. K. Yu, R. Schiff, Y. Li, and R. A, Drezek, *Breast Cancer Research and Treatment,* 125(2011)27-34.

[3] Bartira Rossi-Bergmann, Wallace Pacienza-Lima, Priscyla D. Marcato, Roseli de Conti, and Nelson Durán*, Journal of Nano Research*, 20(2012) 89-97

[4] C. L. Nehl, N. K. Grady, G. P. Goodrich, F. Tam, N. J. Halas, and J. H. Hafner, *Nano Lett.*, 4 (2004)2355-2359.

[5] J. B. Lassiter, J. Aizpurua, L. I. Hernandez, D. W. Brandl, I, Romero, S. Lal, J. H. Hafner, P. Nordlander, and N. J. Halas, *Nano Lett.* 8 (2008)1212-1218.

[6] R. Huschka, A. Barhoumi, Q. Liu, J. A. Roth, J. L, and N. J. Halas, *ACS Nano*. 6 (2012) 7681-7691.

[7] Bohren, C. F. ; Huffman, D. R. *Absorption and Scattering of Light by Small Particles*, Wiley: New York, 1983.

[8] D. W. Mackowski, *Proc. R. Soc. Lond. A* 433(1991) 599-614.
[9] B. Khlebtsov, A. Melnikov, V. Zharov, and N, Khlebtsov. *Nanotechnology* 17(2006) 1437-1445.
[10] R. L. Chern, X. X. Liu, and C. C. Chang, *Phys. Rev. E,* 76(2007) 016609.
[11] D. W. Mackowski and M. I. Mishchenko, *Opt. Soc. Am. A,* 13(2006) 2266-2278.
[12] Y. L. Xu, *Appl. Opt.,* 34(1995) 4573-4588.
[13] Y. L. Xu and N.G. Khlebtsov, *J. Quant. Spectrosc. Rad. Trans.,* 79-80(2003) 1121-1137.
[14] M. A. Yurkin, V. P. Maltsev, A. G. Hoekstra, *J. Quant. Spectrosc. Rad. Trans.,* 106(2007) 546-557.
[15] K. S. Kunz and R. J. Luebbers, *The finite difference time domain method for electromagnetics*; *CRC. Press*, 1993.
[16] A. Kokhanovsky, *Light Scattering Reviews 5*: *Single Light Scattering and Radiative Transfer,* Springer, 2010.
[17] C. Liu and B. Q. Li, *J. Phys. Chem. C*, 115 (2011) 5323-5333.
[18] B. Q. Li and C. Liu, *J. Nanoparticle Research*, 14 (2012) 839-842.
[19] A. Messiah A, *Quantum mechanics*, Dover, New York , 1981.
[20] W. Yang, *Appl. Opt.*, 42 (2003) 1710-1720.
[21] C. L. Nehl, N. K. Grady, G. P. Goodrich, F. Tam, N. J. Halas, and J. H. Hafner, *Nano Lett.*, 4 (2004) 2355–2359.
[22] J. B. Lassiter, J. Aizpurua, L. I. Hernandez, D. W. Brandl, I. Romero, S. Lal, J. H. Hafner, P. Nordlander, and N. J. Halas, *Nano Lett.* 8(2008) 1212-1218.
[23] P. B. Johnson and R. W. Christy, *Phys. Rev. B* 6(1972) 4370.
[24] Kawata, S. *Near-Field Optics and Surface Plasmon Polaritons;* Springer, 2001.

Journal of Nano Research Vol. 23
10.4028/www.scientific.net/JNanoR.23

Energy Absorption in Gold Nanoshells
10.4028/www.scientific.net/JNanoR.23.74